Chapter 2

ENERGETICS AND ADSORPTIONS ON THE NANOTUBE EDGE —Tight-Binding Approaches

2.1 Introduction

The energetics and kinetics are in general two important factors in growth phenomena: Products during atomic reactions evolve into thermodynamically stable forms of NTs, whereas the evolution could be hindered by energy barriers inherent to each atomic reaction. When the energetics is relatively important, the abundant NTs should be thermodynamically stable tubes. On the other hand, when kinetic hindrance is more important, metastable NTs could be abundant.

In this chapter, we discuss those two aspects. First, we determine stable radius and shapes of carbon NTs with finite length. In this task we calculate stable structures of edges and corresponding edge energies. The strain energies of NTs are obtained by the total energy comparison between the graphite sheet and the NT with infinite length. The obtained edge and strain energies are combined to provide the total energy of the finite-length NT as a function of carbon atoms involved. The obtained structural characteristics of the NT edges are principal in discussing atomic reactions during the NT growth.

Second, toward understanding of kinetics such as the adatom diffusion near edges, we here search stable adsorption structures for a single and several carbon adatoms near edges of NTs. These results are fundamental in clarifying growth mechanisms, in particular open growth mechanisms where edges of NTs are open during the growth. Also, energetics in formation of pentagon and hexagon carbon networks at the edges is clarified for a wide range of tube radii. This is important because the pentagon formation is likely to induce closure of open ends of NTs. We find a crossover at some radius: It is shown that for the (5,5)-tube formation of a pair of pentagons is energetically favorable, whereas the hexagon formation is for the (10,10)-tube.

All calculations are performed using a transferable tight-binding (TTB) model proposed by Ho

and coworkers [72, 73]. More accurate calculations based on the density functional theory might be plausible. Yet we are here interested in stable forms of NTs consisting of hundreds of atoms so that the density functional calculations are formidable. On the other hand, the TTB model provides generally reasonable results in particular for carbon systems [74, 75, 76, 77, 78, 79] since the parameters are fitted so as to reproduce several key results from the density functional theory.

2.2 Methods of Calculations

A single wall carbon NT is simulated by a supercell model in which the NT is arranged periodically with a sufficiently large separation of 5.3 Å. To treat a finite-length NT, we place the tube with edges of both sides in a center of a unit cell in the supercell model. When we calculate adsorption of carbon adatoms at an edge of the NT, we terminate the other edge by hydrogen atoms. A geometrical optimization is performed by the conjugate gradient (CG) minimization of the total energy of the system $E_{\rm tot}$ with respect to the atomic configuration.

We use in this chapter the transferable tight-binding model proposed by Ho and his collaborator [72, 73]. In the case of the carbon atom, the atomic orbitals to be considered are $2s$, $2p_x$, $2p_y$ and $2p_z$. In this model, the total energy of the system $E_{\rm tot}$ is

$$E_{\rm tot} = E_{\rm bs} + E_{\rm rep}, \tag{2.1}$$

where the $E_{\rm bs}$ is the energy of the electrons that is the summation of the eigenvalues of the occupied states and the $E_{\rm rep}$ is the ionic repulsive energy. The electronic eigenvalues are obtained by solving the tight-binding Hamiltonian $H_{\rm TB}$.

The tight-binding parameters are determined in order to reproduce structural properties of several carbon polymorphs obtained from the density functional calculations [72]: The energy-volume curves are almost identical to these from the density functional calculations for diamond and graphite, and for other polymorphs. The agreement is satisfactory; The calculated elastic constants and phonon frequencies agree with the experimental values within the error of typically 5%. We adopt the functional forms and the parameters determined in the original work [72]: It has been also established that the present model is capable of describing structural properties of fullerenes and liquid and amorphous carbons quantitatively [74, 75, 76, 77, 78, 79].

Horsfield *et al.* have introduced the parameters for carbon-hydrogen and hydrogen-hydrogen interactions (the ionic repulsions and the electronic hoppings) [80]. They have used the functional forms and the parameters for the carbon-carbon interactions proposed by Ho. The parameters for the carbon-hydrogen and hydrogen-hydrogen interactions have been determined in order that the model is capable of describing bond lengths and total energy differences of hydrocarbons, hydrogenated amorphous carbon systems and hydrogen terminated diamond (100) surfaces. The results obtained by this model agrees satisfactorily with both experimental and *ab initio* results [80, 81]. The parameters for carbon-hydrogen and hydrogen-hydrogen interactions in this thesis are adopted from the work by Horsfield *et al* [80]. (The functional forms of the $E_{\rm bs}$ and $E_{\rm rep}$, and the

tight-binding parameters are given in Appendix C.)

2.3 Energetics of Nanotubes

2.3.1 Strain energy

First we calculate strain energy of the (m,n)-tube, $E_{\rm strain}^{(m,n)}$ ($m = n$ for armchair and $n = 0$ for zigzag). This energy is an energy cost to roll a single graphite sheet into a tubular shape. It is defined as,

$$E_{\rm strain}^{(m,n)} = E_{\rm tot}^{{\rm inf}(m,n)} - E_{\rm tot}^{\rm graphite}, \tag{2.2}$$

where $E_{\rm tot}^{{\rm inf}(m,n)}$ and $E_{\rm tot}^{\rm graphite}$ are total energies per an atom of an infinite-length (m,n)-type NT and a single graphite sheet, respectively. We choose 14 armchair tubes ($n = 4 \sim 13, 15, 18, 20, 24$) and 14 zigzag tubes ($m = 6, 8 \sim 13, 15, 18, 20, 24, 30, 36, 40$). Figure 2.1 shows calculated $E_{\rm strain}^{(m,n)}$ for a variety of NTs. The calculated strain energies are well fitted to a single line defined as

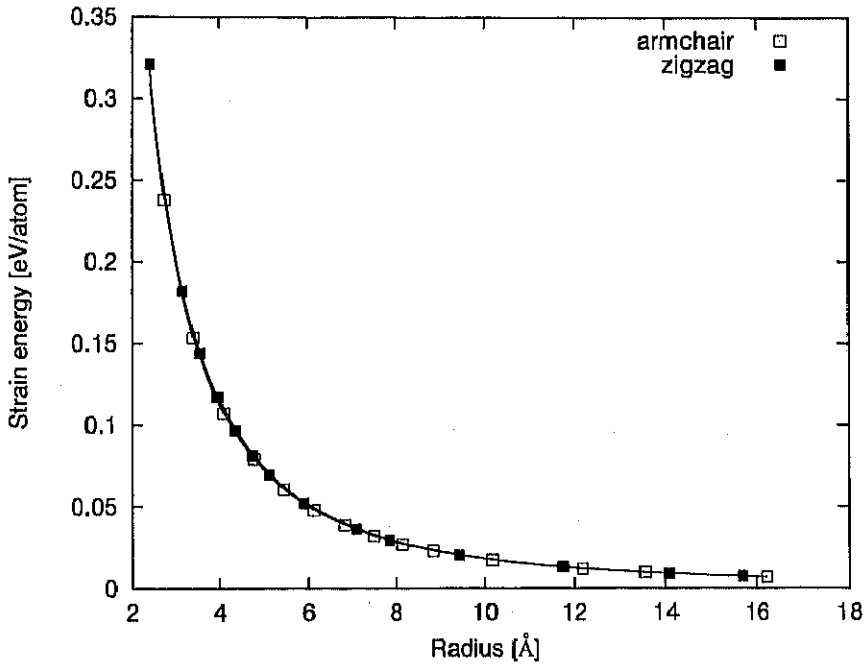

Figure 2.1: Strain energies per atom of the geometrically optimized armchair and zigzag NTs. The energy reference (zero energy) is the energy of a single graphite sheet. Open and solid squares indicate the $E_{\rm strain}^{(m,n)}$ of the armchair NTs and the zigzag NTs, respectively. The solid lines are least-square fitted curves with the form of $A \times ({\rm radius})^{-2}$.

$A \cdot R^{-2}$ where R is a radius of the NT. The coefficient A is obtained as A=1.79 eV Å^2/atom for the armchair NTs and and A=1.84 eV Å^2/atom for the zigzag NTs. The values of the coefficients are in agreement with previous values obtained by the LDA calculations for thinner tubes with the radii of 7 Å or less [82]. We have found a general trend that the strain energy of the armchair

NT is lower than that of the zigzag NT at the same radius. This is interpreted as follows. For the armchair NT, the (n,n)-tube has $N_A = 2n$ atoms on the periphery and the peripheral length is $L = \sqrt{3}an = \frac{\sqrt{3}}{2}aN_A$, where a is the lattice constant of a graphite honeycomb structure. Thus the radius of the armchair NT is related to N_A as

$$N_A = \frac{4\pi}{\sqrt{3}a}R. \tag{2.3}$$

Similarly, for the zigzag NT, a number of atoms N_Z on the periphery is

$$N_Z = \frac{2\pi}{a}R. \tag{2.4}$$

Accordingly N_A is larger than N_Z at the same radius. If the strain energy depends only on the radius of NT, the strain energy per atom of the armchair NT is smaller than that of the zigzag NT. Yet the energy difference is very small and the strain energies for both the armchair and the zigzag NTs become zero in the large radius limit.

2.3.2 Edge energy

A NT with finite length has the edge on one end or both ends. In this subsection the edge energy $E_{\rm edge}^{(m,n)}$ which is an energy cost for the edge formation is calculated. This $E_{\rm edge}^{(m,n)}$ is defined as

$$E_{\rm edge}^{(m,n)} = [E_{\rm tot}^{\rm finite(m,n)} \cdot N^{(m,n)} - E_{\rm tot}^{\rm inf(m,n)} \cdot N^{(m,n)}]/N_{\rm edge}^{(m,n)}, \tag{2.5}$$

where $E_{\rm tot}^{\rm finite(m,n)}$ and $N^{(m,n)}$ are a total energy per an atom and a number of atoms of the (m,n)-tube with finite length [1], respectively, and $N_{\rm edge}^{(m,n)}$ is a number of atoms on the edges of the (m,n)-tube with finite length. The edge is regarded as a "surface" of NTs. Some dangling bonds (DB) appear and "surface relaxation" occurs to lower the edge energy. Only flat edges are considered in this subsection. Effects of atomic steps at the edges are considered in the following chapter. We use an armchair tube with the length of 10 atomic rows (This tube is termed as the "10-row-length armchair tube" in short.) and a 12-row-length zigzag tube. Fig. 2.2. These two tubes are representatives for the two types of NTs and are used to evaluate the edge energies. At these sizes of the NTs, $E_{\rm edge}^{(m,n)}$ and an edge bond length are converged in 0.05 eV and 0.05 Å, respectively, with respect to a number of rows. This dependence of $E_{\rm edge}^{(m,n)}$ and the bond length with respect to a number of rows are checked with (5,5)- and (9,0)-tubes. Calculated edge energies per edge atom both for the armchair NTs and the zigzag NTs are shown in Fig. 2.3. (There are $4n$ edge atoms in the (n,n)-tube, whereas $2n$ edge atoms in the $(n,0)$-tube.) It is found that the edge energies of the armchair NTs are substantially lower than those of the zigzag NTs for any value of the tube radius. The energy difference is ~ 0.5 eV/edge atom. When we neglect relaxation of atoms near the edge, the edge energy may be roughly proportional to the number of DBs generated at the edge. Hence the edge energy per edge atom, which is the same to the edge energy per DB

[1] In this subsection, a fixed number of $N^{(m,n)}$ is used to calculate the $E_{\rm tot}^{\rm finite(m,n)}$ and $E_{\rm edge}^{(m,n)}$. This $N^{(m,n)}$ is sufficiently large to calculates the $E_{\rm edge}^{(m,n)}$. (See text.) In §2.3.3, this number of atoms is used as a variable.

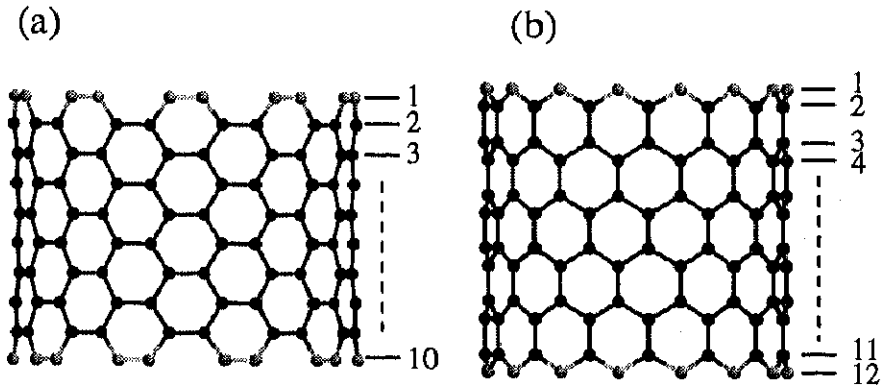

Figure 2.2: Side views of NTs with finite length used for calculations of edge formation energies. (a) An armchair NT is constructed from 10 rows. The (n, n)-tube here has $20n$ atoms in total and $4n$ atoms on the edge. (b) A zigzag NT is constructed from 12 rows. The $(n, 0)$-tube here has $12n$ atoms in total and $2n$ atoms on the edge. Atoms on the edge are depicted by lighter spheres.

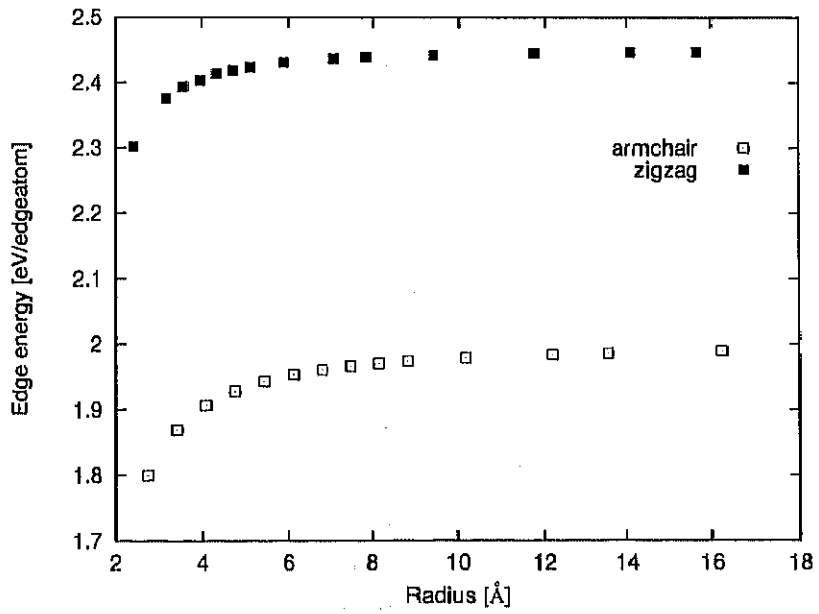

Figure 2.3: Edge formation energy per edge atom of the geometrically optimized armchair and zigzag NTs with finite lengths. Open and solid squares indicate the $E_{\rm edge}^{(m,n)}$ of the armchair and zigzag NTs, respectively.

at the unrelaxed edge, is insensitive to the structure of NT. The energy difference of 0.5 eV that we have found is therefore purely due to the relaxation of edge atoms. For the armchair NT, the DBs are stabilized by the π interaction with adjacent DBs. In fact, we have found that the bond length at the edge is substantially shortened and is $\sim$1.2 Å that is close to the length of the triple bond in acetylene. This triple bond formation is "a surface relaxation" of the armchair NT. On the other hand, for the zigzag NT the interaction between DBs is weak due to the longer distance between adjacent DBs.

This higher edge energies of the zigzag NTs indicate that the zigzag NTs are likely to be closed. This is in accord with the previous result that an energy gain of a cap formation on the zigzag edge is larger than the case for the armchair edge [66]. The edge relaxation to stabilize DBs introduces the lattice distortion. The edge energies contain an effect of this distortion. This effect become relatively small on the edge of the thin NT which is already distorted by its high curvature. Therefore, the edge energy decreases in the region of the small radius.

2.3.3 Total energy of finite-length nanotubes

Combining the strain energy and the edge energy calculated in the previous subsections, we obtain the total energy of NTs with finite length. When the (m,n)-tube consists of N carbon atoms, its total energy with respect to a flat graphite sheet of N atoms can be calculated by,

$$E_{\rm tot}^{(m,n)} = E_{\rm strain}^{(m,n)} \cdot N + E_{\rm edge}^{(m,n)} \cdot N_{\rm edge}^{(m,n)}, \tag{2.6}$$

where $N_{\rm edge}^{(m,n)}$ is a number of atoms on the edges of the (m,n)-tube with finite length, and $E_{\rm strain}^{(m,n)}$ and $E_{\rm edge}^{(m,n)}$ are already calculated in the previous subsections. When the number of carbon atoms N is fixed, we can construct several kinds of NTs, from a thick and short tube to a thin and long tube. The thick and short tubes have higher edge energy since this tube has more edge atoms. On the contrary, the thin and long tubes have larger strain energy. Therefore, due to the competition of $E_{\rm strain}^{(m,n)}$ and $E_{\rm edge}^{(m,n)}$, an optimized size (radius and length) of the NT at each N is expected. This consideration is illustrated in Fig. 2.4. From the results of §2.3.1 and §2.3.2, the R^{-2} and R^{1} behaviors are assumed for the $E_{\rm strain}^{(m,n)}$ and the $E_{\rm edge}^{(m,n)}$, respectively, where R is the radius of the NT. The total energy $E_{\rm tot}^{(m,n)}$ as a summation of the $E_{\rm strain}^{(m,n)}$ and the $E_{\rm edge}^{(m,n)}$ is indicated by a dushed line in Fig. 2.4. Since the $E_{\rm strain}^{(m,n)}$ is dominant in the small radius limit, it is expected that the $E_{\rm tot}^{(m,n)}$ is proportional to R^{-2}. On the other hand, in the large radius limit, it is expected that the $E_{\rm tot}^{(m,n)}$ is proportional to R. Calculated $E_{\rm tot}^{(m,n)}$ as a function of the radius is shown in Fig. 2.5 for N =1000 (squares) and 2000 (circles). We have found that the armchair NT is energetically favorable compared with the zigzag NT for $N = 1000$ and $N = 2000$. The optimized NTs that have the minimum total energies are $(12,12)$ and $(15,15)$ for N =1000 and 2000, respectively. It is also found that the shape of the plots are similar to the behavior of the $E_{\rm tot}^{(m,n)}$ expected in Fig. 2.4. We plot the $E_{\rm tot}^{(m,n)}$ as a function of the number of atoms in Fig. 2.6. It is found that the most stable NTs are always of armchair type. This stability of the armchair NTs is due to the small edge energy owing to the efficient π interactions. The radius of the most stable NT increases with

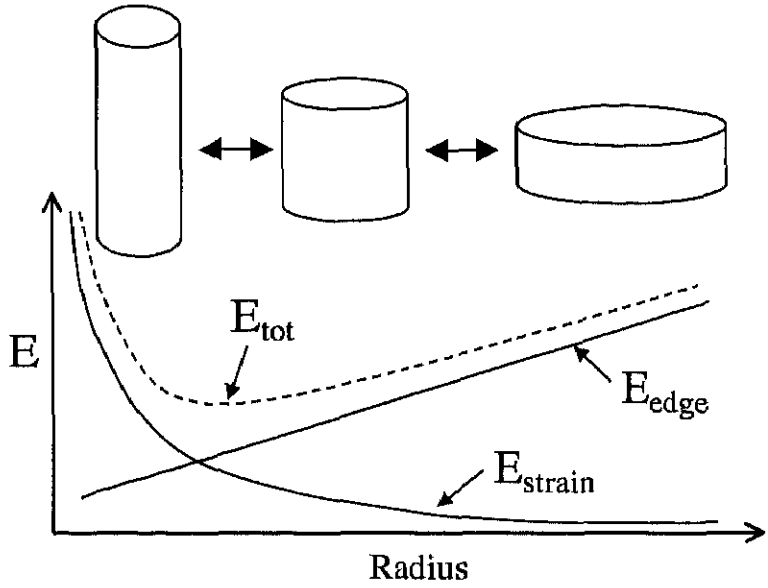

Figure 2.4: Schematic diagrams illustrating the energetics of the finite-length NT. When the number of the atom is fixed, we can construct several kinds of the NTs, from a (relatively) thin and long tube to a thick and short tube. (Upper figures. The chirarity is not considered here.) The lower figures show the radius dependences of the $E_{\rm strain}$, $E_{\rm edge}$ and $E_{\rm tot}$. From the results of the previously subsections, the $E_{\rm strain}$ ($E_{\rm edge}$) can be expected to behave as R^{-2} (R). The dushed line indicates the $E_{\rm tot}$ as a summation of the $E_{\rm strain}$ and the $E_{\rm edge}$. (Superscripts "(m,n)" are omitted here for simplicity.)

increasing N. In Fig. 2.6, only four armchair NTs are plotted. Yet actually the most stable tube varies as $\cdots \rightarrow (10,10) \rightarrow (11,11) \rightarrow (12,12) \rightarrow \cdots$ around $N = 1000 \sim 2000$. When N become large relative to $N_{\rm edge}^{(m,n)}$, the effect of the edge is relatively small and the strain energy become dominant. Therefore, at large N the thick tube is energetically preferred.

When the number of atoms N changes continuously from 1000 to 2000, several NTs are unable to possess flat edges and the steps inevitably appears at the edge. We have neglected the effect of such steps in this subsection, however, to obtain gross features of the energetics of NTs with finite length.

Furthermore, the length of the most stable NT L is considered here. The most stable NT has been already obtained in Fig. 2.6. The length of the finite-length NT is determined from N and the index of the NT. Therefore, we can derive the length of the most stable NT as a function of N *i.e.* $L(N)$. Figure 2.7 indicates this length. We consider also the (8,8), (12,12) and (18,18) tubes in addition to the (5,5), (10,10), (15,15) and (20,20) tubes. The solid line in Fig. 2.7 indicates $L(N) = 0.619N^{\frac{2}{3}}$, which is fitted to the calculated length satisfactorily. This function can be derived analytically from Eq.(2.6). The derivation is follows. (We consider only the armchair NTs because the armchair NTs are always more stable than the zigzag NTs.) The strain energy has been obtained as $E_{\rm strain}^{(n,n)} = 1.79/R^2$ eV/atom for the armchair NT. Since we consider the flat edge, the $N_{\rm edge}^{(n,n)}$ is equal to $2N_A$, where the N_A is the number of the atoms on the periphery of the

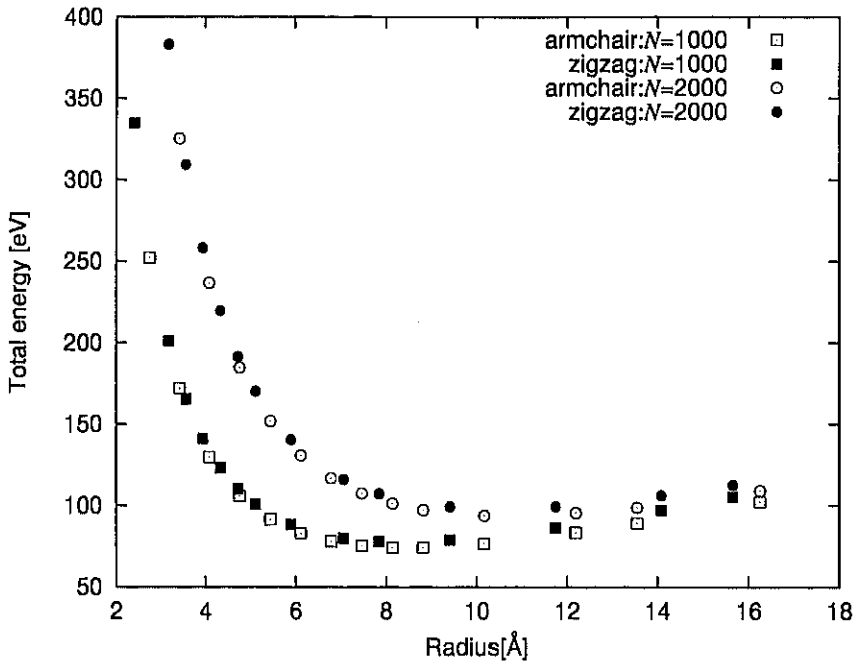

Figure 2.5: The total energy of a NT with finite length $E_{\rm tot}^{(m,n)}$ at N =1000 and 2000 as a function of the nanotube radius. The energy reference is the total energy of a flat graphite sheet. Open squares and circles indicate $E_{\rm tot}^{(n,n)}$ of the armchair NTs at N =1000 and 2000, respectively. Solid squares and circles indicate $E_{\rm tot}^{(n,0)}$ of the zigzag NTs at N =1000 and 2000, respectively. $E_{\rm strain}^{(m,n)}$ decreases and $E_{\rm edge}^{(m,n)}$ increases with increasing radius. Thus, a concave shape of plots is obtained. In both cases of N =1000 and 2000, the total energy of the armchair NT is lower than that of the zigzag NT. The tube that has the minimum total energy is (12,12) (R=8.1 Å) for N=1000 and (15,15) (R=10.2 Å) for N=2000.

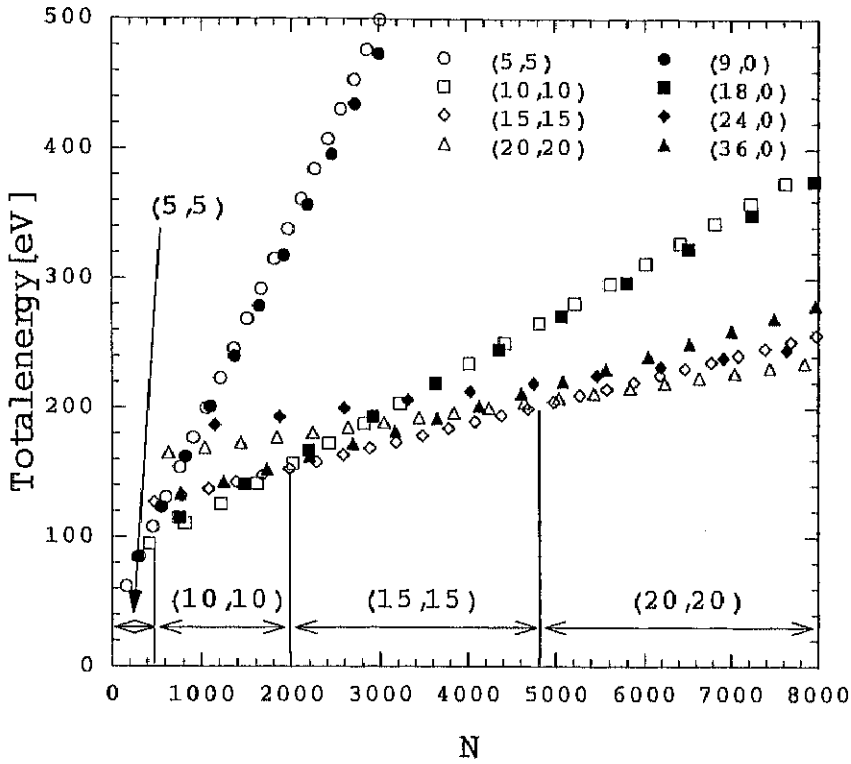

Figure 2.6: The total energy of a NT with finite length with respect to a flat graphite sheet as a function of N. We pick up eight kinds of NT from the armchair type, $(5,5) \sim (20,20)$, and from the zigzag type, $(9,0) \sim (36,0)$. The most stable tube is always of armchair type and its radius increases with increasing N. The most stable tube and its range of N are also indicated.

armchair tube. (See Eq.(2.3).) The factor 2 originates from that the finite-length NT has two edges. Therefore, the $E_{\rm tot}^{(n,n)}$ is rewritten as,

$$E_{\rm tot}^{(n,n)} = \frac{1.79}{R^2}N + E_{\rm edge}^{(n,n)}\frac{8\pi}{\sqrt{3}a}R. \tag{2.7}$$

On the other hand, the number of atoms is given as

$$N = \frac{2\pi RL}{s}, \tag{2.8}$$

where $s = \frac{\sqrt{3}a^2}{4}$ is an area that one carbon atom occupies in the graphite sheet. Thus, the R is represented by the N as

$$R = \frac{\sqrt{3}a^2}{8\pi L}N. \tag{2.9}$$

Substituting Eq.(2.9) into Eq.(2.7), we obtain the total energy as a function of the L and N:

$$E_{\rm tot}^{(n,n)}(L,N) = 1.79\left(\frac{8\pi}{\sqrt{3}a^2}\right)^2 \cdot \frac{L^2}{N} + E_{\rm edge}^{(n,n)}a\frac{L}{N}. \tag{2.10}$$

The length of the most stable NT is derived from a condition

$$\left(\frac{\partial E_{\rm tot}^{(n,n)}}{\partial L}\right)_N = 0. \tag{2.11}$$

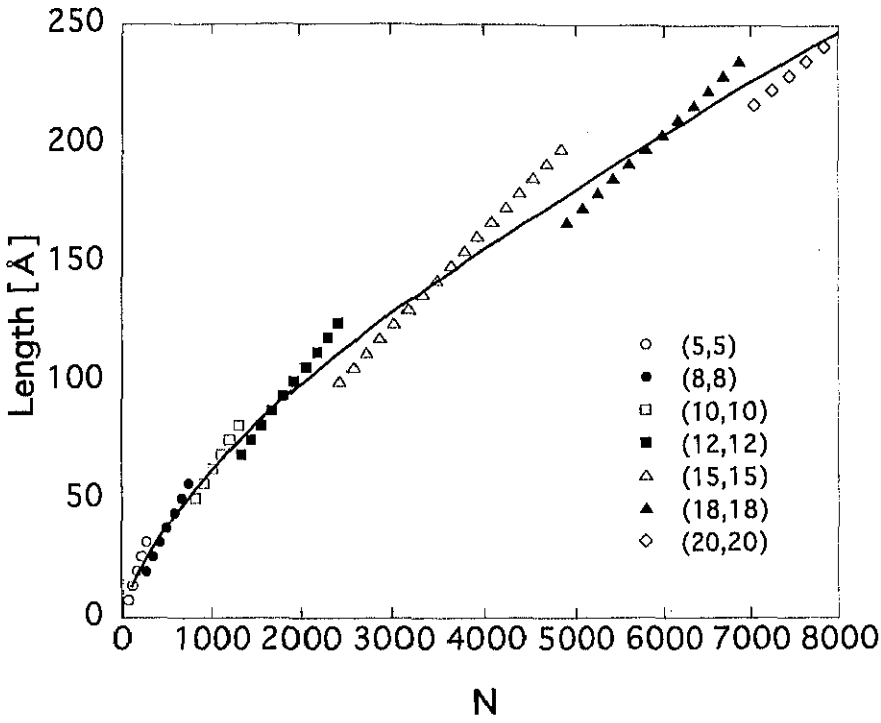

Figure 2.7: The length of the most stable NT is indicated as a function of N. We pick up 7 kinds of armchair NTs for calculation. The lengths are calculated only in the range of N that the corresponding NT is most stable. For example, the (10,10)-tube is most stable around N=1000, Generally speaking, the length of the most stable NT increases with increasing N. The solid line indicates the analytic function $L(N) = 0.619N^{\frac{2}{3}}$. (See text.) This analytic function is fitted satisfactorily to the results calculated for each armchair NT.

This derivative of $E_{\rm tot}^{(n,n)}$ with respect to the L is calculated at fixed N. Accordingly, the L is derived as a function of N:

$$2 \cdot 1.79 \left(\frac{8\pi}{\sqrt{3}a^2} \right)^2 \cdot \frac{L}{N} = \frac{E_{\rm edge}^{(n,n)} a}{L^2}$$

$$\iff \quad L = \left[\frac{E_{\rm edge}^{(n,n)} a}{2 \cdot 1.79} \left(\frac{\sqrt{3}a^2}{8\pi} \right)^2 \right] N^{\frac{2}{3}}. \tag{2.12}$$

Using a=2.46 Å and $E_{\rm edge}^{(n,n)}$=1.98 eV,[2] Eq.(2.12) becomes

$$L = 0.619 N^{\frac{2}{3}}. \tag{2.13}$$

Thus, the analytic form of the $L(N)$ for the armchair NTs is obtained.

2.4 Adsorption on the Nanotube Edge

We consider adsorption energies for carbon adatoms at the NT edges in this section. It is found that the armchair NT is energetically favorable compared with the zigzag NT in the previous

[2]Although the $E_{\rm edge}^{(n,n)}$ depends on the R as indicated in Fig. 2.3, the constant $E_{\rm edge}^{(n,n)}$ (=1.98 eV) is used for all armchair NTs for simplicity.

section. Hence we concentrate on the adatom adsorption on the armchair NTs.

We use (n,n)-tubes ($n = 5 \sim 24$) with 8 atomic rows length to calculate adsorption sites and adsorption energies. The adsorption energy $E_{\rm ad}$ is defined as

$$E_{\rm ad} = \left[E_{\rm tot}(N) + N_{\rm ad} \cdot E_{\rm atom} - E_{\rm tot}(N + N_{\rm ad})\right]/N_{\rm ad}, \tag{2.14}$$

where N and $E_{\rm tot}(N)$ are the number of the carbon atoms and the total energy of the NT without adatom, respectively, $N_{\rm ad}$ is the number of the carbon adatom, $E_{\rm atom}$ is the energy of the carbon atom and $E_{\rm tot}(N + N_{\rm ad})$ is the total energy of the NT on which the $N_{\rm ad}$ adatoms are adsorbed. In this work, $N_{\rm ad}$ varies from 1 to 4. Adatoms are adsorbed on a top edge of the NT. A bottom edge is terminated with hydrogen atoms and fixed during a geometrical optimization to simulate an infinite-length NT. The dependence of the adsorption energy and the edge bond length with respect to a number of rows are checked with the (10,10)-tube. It is found that the adsorption energy and the edge bond length are converged in 0.01 eV and 0.01 Å, respectively, with respect to the number of rows already at the the 8-row-length NT. In the following subsections, we discuss the adsorption energies of carbon adatoms at several sites on the flat edges, formation energies of a set of pentagon networks and hexagon networks at the edges, and an effect of the pentagon network on the following adsorption processes.

2.4.1 Flat edge

We consider here the fundamental adsorption structures on the armchair edge, that is, pentagon and hexagon network. [3] When the single adatom is adsorbed on the site between the triple bonds (This site is termed as the "seat site".), the pentagon network is formed as shown in Fig. 2.8 (a). The two triple bonds between the atom marked as 1 (atom-1) and the atom-2 and between the atom-3 and the atom-4 in Fig. 2.8 (a) nearby the pentagon network are therefore weakened: The bond lengths are $\sim$ 1.4 Å, which is close to the length of the C−C bond in benzene. Upon the adatom adsorption, characters of dangling bonds thus come up at the atoms 1 and 4 in Fig. 2.8 (a), along with the DB at the adatom.

We next put an additional carbon atom on the edge (2 adatoms in total). The stable structure is shown in Fig. 2.8 (b). A hexagon network is formed above the seat site. Again, the triple bonds between the atom-1 and the atom-2 and between the atom-3 and the atom-4 nearby in Fig. 2.8 (b) nearby the hexagon network are weakened and then the dangling bond characters come up on the atom-1 and atom-4. On the other hand, the bond at the new hexagon has a character of the triple bond: The bond length is 1.28 Å. When we compare the two structures in Fig. 2.8, the hexagon

[3] Several adsorption structures on the flat armchair edge can be considered. For example, if the single adatom is adsorbed just above the triple bond (This site termed as the "arm site".), the triangle network is formed (See Fig. 3.4 (a).). Unfortunately, since the parameters of the TTB are fitted to reproduce the energy of the typical structure, such as the graphite and the diamond, the energy of the triangle network which is largely distorted from the ideal sp^2 bonding cannot be estimated precisely by the TTB. Thus, only the pentagon and hexagon network on the armchair edge are considered here. The other adsorption structures are investigated in chapter 3 by the LDA calculations.

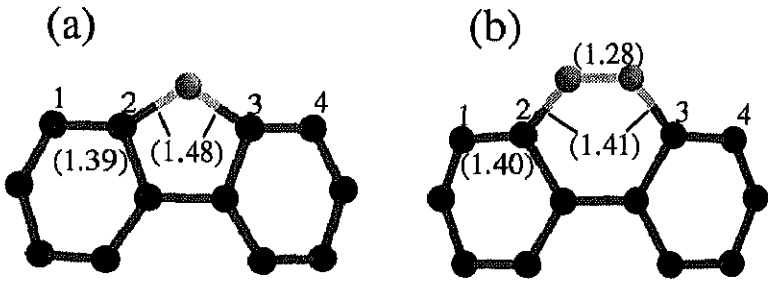

Figure 2.8: Side views of geometrically optimized pentagon and hexagon network on the armchair edge. Only top four rows and adatoms are depicted. Adatoms are indicated by lighter spheres. Numbers of $1 \sim 4$ are atom indexes. Values in parentheses indicate the bond lengths in Å.

formation is likely to be energetically favorable since the additional DB exists in the pentagon structure.

This can be quantified by comparing the adsorption energies. Then, we consider a dependence of the adsorption energy with respect to the NT radius. The adsorption energies of the pentagon and hexagon are plotted in Fig. 2.9. Although the adsorption energy of the hexagon is almost independent with respect to the radius, that of the pentagon decreased with increasing radius. Consequently, the pentagon is more stable in a smaller radius NT. When we consider the growth of NTs with open edges, formation of pentagon arrays at edges induces closure of the edges and hereby prevents the tube growth. It is thus of interest to compare energies of several pentagons and of hexagons at edges. We here consider formation energies of two pentagons and one hexagon and those of 4 pentagons and two hexagons at the armchair edge as shown in Fig. 2.10. Calculated energies are shown in Fig. 2.11. In general the energy of the pentagon array increases with increasing radius of NTs. This is due to the fact that the lattice distortion around the pentagon becomes prominent for thicker NTs where the carbon walls are more flat than the thinner NTs. We have found a crossover of the radius at which the hexagon formation becomes energetically favorable than the pentagon formation. The open edge growth is thus likely for thicker NTs.

2.4.2 Roles of a pentagon

Adsorption on the flat edge is discussed so far. During the open growth of a NT, there should be several adatoms on its edge and the several pentagons and hexagons are presumably formed on the edge. In this subsection, in order to clarify roles of the pentagon during the growth, we study effects of the pre-adsorbed pentagon on the adsorption of additional carbon atoms. We first prepare a pentagon (a pre-adsorbed pentagon) on the flat edge to investigate the effect of this pentagon. We then explore adsorption sites for the additional atom around the pre-adsorbed pentagon and calculate the corresponding adsorption energy $E_{\rm ad}^{\rm pen}$. We define $E_{\rm ad}^{\rm pen}$ as,

$$E_{\rm ad}^{\rm pen} = -E_{\rm tot}^{\rm pen+adatom} + E_{\rm tot}^{\rm pen} + E_{\rm atom}, \tag{2.15}$$

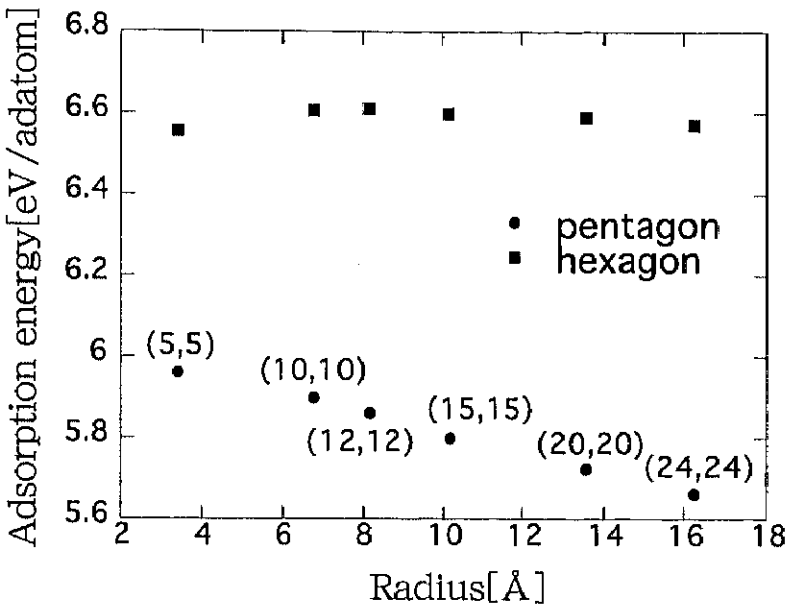

Figure 2.9: Adsorption energies on the armchair((5,5), (10,10), (12,12), (15,15), (20,20) and (24,24)) edges. Solid circles and squares indicate the energies of the pentagon and hexagon network on the armchair edge, respectively.

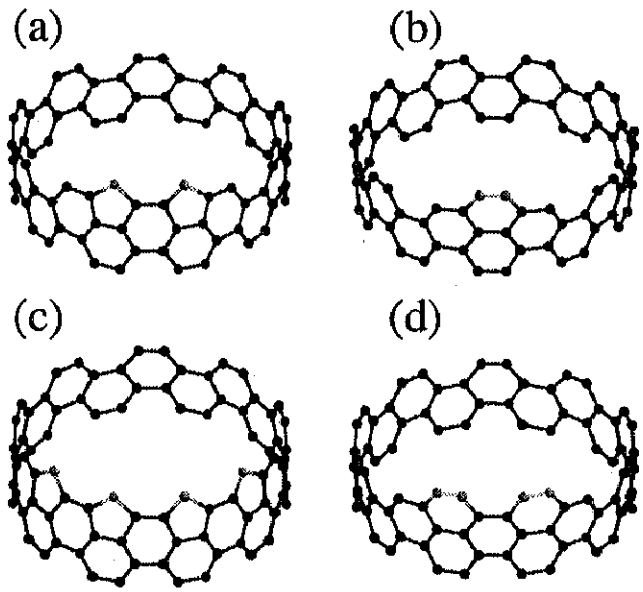

Figure 2.10: Structures of the geometrically optimized (10,10) edge with two or four adatoms. Only top 4 rows and adatoms are depicted. Adatoms are represented by lighter spheres. (a) Two adatoms form two-pentagon array. (b) Two adatoms form a hexagon. (c) Four adatoms form four-pentagon array. (d) Four adatoms form two-hexagon array. We construct similar structures on edges of the (5,5), (10,10) and (20,20) tubes to calculate the adsorption energies for each case.

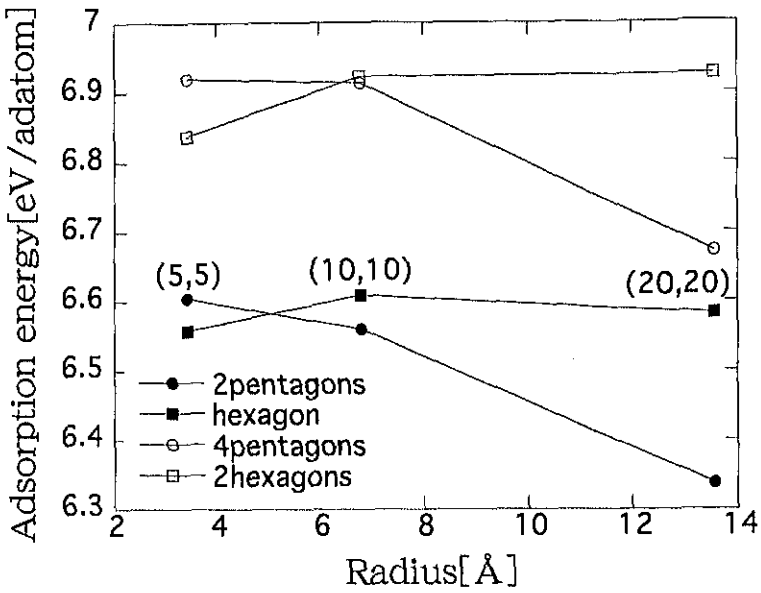

Figure 2.11: Adsorption energies of two pentagons, a hexagon, four pentagons and two hexagons on (5,5), (10,10) and (20,20) edge as a function of radius. The solid line is only a guide for eyes. For both cases of two and four pentagons, the adsorption energy decreases with increasing radius. The pentagon has high energy on the edge of the large radius NTs.

where $E_{\rm tot}^{\rm pen+adatom}$ is a total energy of the NT with the pre-adsorbed pentagon plus the additional adatom, $E_{\rm tot}^{\rm pen}$ is a total energy of the NT with the pre-adsorbed pentagon and $E_{\rm atom}$ is an energy of the carbon atom. Each structure and the corresponding adsorption energy are summarized in Fig. 2.12, where the additional adatom is highlighted with a lighter sphere and "5" indicates the position of the pre-adsorbed pentagon. The number of "6" in Fig. 2.12 indicates the hexagon transformed from the pre-adsorbed pentagon by incorporation of the additional adatom.

In Fig. 2.12 (a), additional adatom is incorporated to the pre-adsorbed pentagon, followed by that this pentagon is transformed to the hexagon network.[4] In Fig. 2.12 (b), the additional adatom is adsorbed on the nearest seat site of the pre-adsorbed pentagon, and a two-pentagon array is formed. The hexagon is energetically more favorable than the pentagon array on the (10,10) edge as discussed previously. However, in Fig. 2.12 (b), since the additional adatom erases a DB generated by the pre-adsorbed pentagon, the adsorption energy is larger than that of the seat site adsorption with no other adatoms. On the next nearest seat site of the pre-adsorbed pentagon, the effect of the pre-adsorbed pentagon becomes already small: The adsorption energy of this site is almost equal to that on the flat edge with no other adatom. In the case of the two-pentagon array (Fig. 2.12 (b)), there are four DBs. (DBs are on the adatoms and the nearby seat sites.) On

[4]Actually, some activation energy is required to incorporate the additional adatom into the pre-adsorbed pentagon. However, we neglect here this activation energy and obtain the corresponding adsorption energy from the total energy of the NT with hexagon network. (The total energy of the NT with hexagon network is substituted into the $E_{\rm tot}^{\rm pen+adatom}$ in Eq. (2.15).)

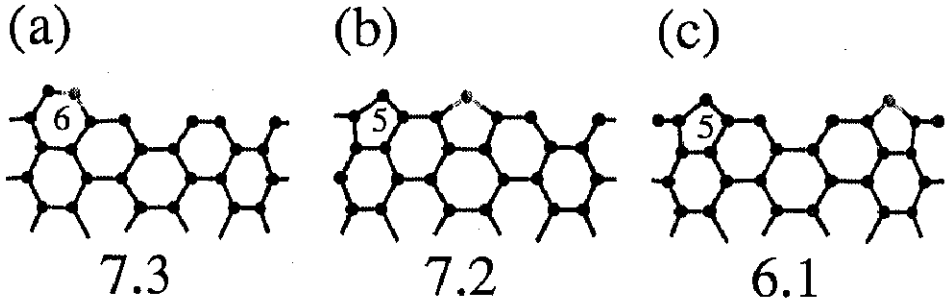

Figure 2.12: Side views of the geometrically optimized edge structures with a pre-adsorbed pentagon plus an additional carbon atom. Values below the each side view are adsorption energies in eV. The additional adatom is depicted by a lighter sphere. The pentagon marked as "5" is the pre-adsorbed pentagon and the hexagon marked as "6" is the hexagon transformed from the pre-adsorbed pentagon by incorporation of the additional adatom. (a)~(c) Flat edge. (a) The additional adatom is incorporated to the pre-adsorbed pentagon, followed by that the hexagon network is formed. (b) The additional adatom is adsorbed on the nearest seat site of the pre-adsorbed pentagon and the two-pentagon array is formed.

the other hand, when the two pentagons are separated by more than one seat site, three DBs are generated by each pentagon. Thus, there are six DBs on the edge shown in Fig. 2.12 (c). From the viewpoint of the DB counting, the two-pentagon array is more favorable than other arrangements of pentagons.

In short, the calculation of the adsorption energies in this subsection indicates that, the hexagon network formation and the pentagon on the nearest seat site of the pre-adsorbed pentagon are energetically favorable. The nearest seat sites of the pre-adsorbed pentagon become sinks for the additional adatom because of the DBs generated by the pre-adsorbed pentagon. This effect is quite local in a sense that the adsorption on other sites are not affected from the pre-adsorbed pentagon. It is thus of interest that the pentagon has an ambivalent character: It suppresses the growth by triggering the cap formation, but at the same time becomes a nucleation site for additional atoms and hereby accelerates the hexagon formation.

2.5 Summury

In this chapter, to clarify the energetics of the NT, we have calculated the strain energy, the edge formation energy and the total energy of the finite-length NT. The strain energy of the armchair NT is found to be lower than that of the zigzag NT at the same radius. For the edge formation energy, we have found that the armchair edge is more stable than the zigzag edge because of the triple bond formation at the armchair edge. The total energy of the finite-length NT has been calculated as a function of the number of constituting carbon atoms N from the combination of the strain energy and the edge energy. The most stable NT is always armchair type and become thicker with increasing N. These results of energetics suggest that the armchair tube are formed and grow to a long NT more easily than the zigzag tube. The calculation of adsorption energy

has been also performed. The energetics of a pentagon and a hexagon on the armchair flat edge is discussed. It has been found that the energy of the pentagon increases with increasing the NT radius. The pentagon network is more stable on the edges of thin NTs than the hexagon network which maintains open growth, suggesting that the thin NT is not favorable for the open edge growth. We have discussed the effect of the pentagon to the additional adatom adsorption. The adsorption on the nearest seat site of the pre-adsorbed pentagon is energetically favorable along with the hexagon network formation by incorporation of the additional adatom to the pre-adsorbed pentagon.